ACTA MONTANA IRSM AS CR (1999)
Series A No.14 (114), 39–54

ENERGY OF SEISMIC WAVES RADIATED BY FINITE CIRCULAR SOURCE — NUMERICAL APPROACH

PETR KOLÁŘ

Geophysical Institute, Academy of Sciences of the Czech Republic
Boční II, Prague 4 – Spořilov, 141 31, Czech Republic (e-mail: kolar@ig.cas.cz)

ABSTRACT. We used a method, which allowed determined energy radiated in seismic waves from a seismogram recorded at one station only. In present work we compared how the results can differ if final source was neglected and replaced by a point source. The investigation was performed by numerical experiments. To be able to evaluate synthetic seismograms we developed a suitable model of the kinematic finite circular source. We investigated the influence of *take-off angle*, *distance*, *rake* and *rupture velocity*. We found that omitting a finite source can affects a final seismic energy, but the difference is less than an order of magnitude. The influence of the *take-off angle* was found to be the most significant, the influence of other investigated parameters (*distance*, *rake*, *rupture velocity*) is of less importance. The dependency of determined energy on *take-off angle* is monotonous in general, however some irregularities for S waves energy were discovered.

KEYWORDS: Seismic energy determination, finite circular source.

1. INTRODUCTION

In my previous works I determined the energy radiated in seismic waves for real earthquakes from seismograms recorded at only one seismic station (Kolář, 1994a; b). At those
the results can differ if a final source (circular source in our case) is consider. The problem is studied

The energy was calculated
icyn (1915), later used and modified several times, e.g. by Boatwright (1980). Let me briefly describe the method: first, the energy flow in a point of observation (i.e. at
gram. Then we move from the station to the sour
path effect (geometrical
on focal sphere in one particular direction. Under the assumption of a source type we can then
as a sum of energies radiated in all directions; in other words, the energy flux is integrated over the whole focal sphere. The influence of the radiation pattern, source

type, etc. must be considered. The method can be described by the formula

$$E^c = \frac{4\pi \left\langle \left(F^c\right)^2 \right\rangle (v_c \rho)}{G^2 A^2 \left(F^c(\nu,\varphi)\right)^2 \left(K^c\right)^2} \int_{t_{c_1}}^{t_{c_2}} \left(v(\boldsymbol{x},t)\right)^2 \mathrm{d}t \,, \tag{1}$$

where E stands for energy, c for P or S wave and v_c is the wave velocity, $F^c(\nu,\varphi)$ is the value of the radiation
the ray
of $\left(F^c(\nu,\varphi)\right)^2$ over the whole focal sphere (value of $\left\langle (F^c)^2 \right\rangle$ is given
and
the
boundaries), A is the absorption factor, K^c is the conversion coeficient of the free surface,
and t_{c_2} determine
that
works properly only if the energy flux is calculated from records of direct waves (P and/or S). Formula (1) incorporates all important influences, which affect seismic waves during their generation and propagation. The velocity $v(\boldsymbol{x},t)$ must be naturally a real ground velocity
must be corrected if necessary.
source. The method allows us in principle to calculate the total energy radiated in seismic waves
however, many other information
source location, source type and mechanism, etc.).

The present work deals with only one particular problem of the method: during t
influence of a finite seismic source
results given by Boatwright (1980). Present study shows how the value of calculated seismic energy radiated
waves are generat
was performed by using numerical simulations and we supposed a circular type
a finite source. Synthetic seismogram
for various points of observations and for various values of investiga
(take–off angle, dist rake). Then the seismic energies
were det — i.e.
assumption of a point seismic source model. The relative changes of seismic energy caused by uncorrected influence of a finite seismic source were observed in dependence on the investigated parameters.

The calculations were performed for synt
vestigated parameters rce and a station, diameters of a
finite source etc.) were inspired by real
(Kolář, 1992; 1994a; b).

2. Finite Source Model

For the calculation of synthetic seismograms I assumed a planar circular source of

double–couple type. Such source is widely used for modelling of small earthquakes — see e.g. Antonini (1987). The finite source was
of point sub–sources or, in fact, the final seismogram was calculated as a sum of seismograms radiated by individual point sub–sources. For the calculation we have to be able evaluate course of displacement
quoted also as sub–STF) in every point of the source, we have to also prescribed somehow distribution of sub–sources on the fault.

The source model here described is inspired by the work of Madariaga (1976), namely by figure 3 of quoted work. The sub–sources are distributed inside the circular fault
that there is a grid point in the centre of the circle — see Fig. 1. The density of the grid (the distance l between two closest point sources) is given as the fraction of the radius of the circle. All sub–sources are of the same mechanism (i.e. the same strike, dip, rake) and the same shape of the sub–source time function but with different starting times, amplitudes and durations in general. The rupture process starts at the centre of the circle and spreads in all directions with the same rupture velocity v_r. When the rupture front reaches a sub–source, the sub–source starts to radiate with a prescribed sub–source time function. When the rupture front arrives at the fault border, it reflects back and returns to the centre as a stopping front. A schematic example of time variation of a displacement course on the fault is given in Fig. 2.

The sub–source time function is designed in the following
slip (displacement) correspond to the rectangular course of sub–source time function — see Fig. 3, curves a, b. To obtain smoother course of the sub–STF we used curve d, which is described as one period of $\sin^2 t$, instead of rectangular one. The corresponding course of the slip is in Fig. 3, curve
is used as a sub–source t
sub–source is fully determined
and an amplitude. The amplitude B corresponds to the maximum value of the slip velocity at a sub–source. The maximum amplitude B_0
In direction to the borders of the source the amplitude B decrease according to the formula

$$B = B_0 \left(1 - \frac{s}{a}\right)^2 , \tag{2a}$$

where s is the distance of the sub–source from the centre and a is the final source radius. The time of duration
rupture
w_{nk} observed at point S_n generated by

$$w_{nk} = \begin{cases} \dfrac{B}{d_{nk}} \sin^2 \left(\dfrac{t - v_c/d_{nk}}{t_{\mathrm{dur}}} \right) F^c(\nu_{nk}, \varphi_{nk}) & \text{for } t_1 \le t \le t_{\mathrm{dur}} \\ 0 & \text{otherwise} . \end{cases} \tag{2b}$$

where d_{nk}, ν_{nk} and φ_{nk} are actual values for d, ν and φ for the particular sub–source k and point of observation S_n. The final seismogram in S_n is then given as a sum

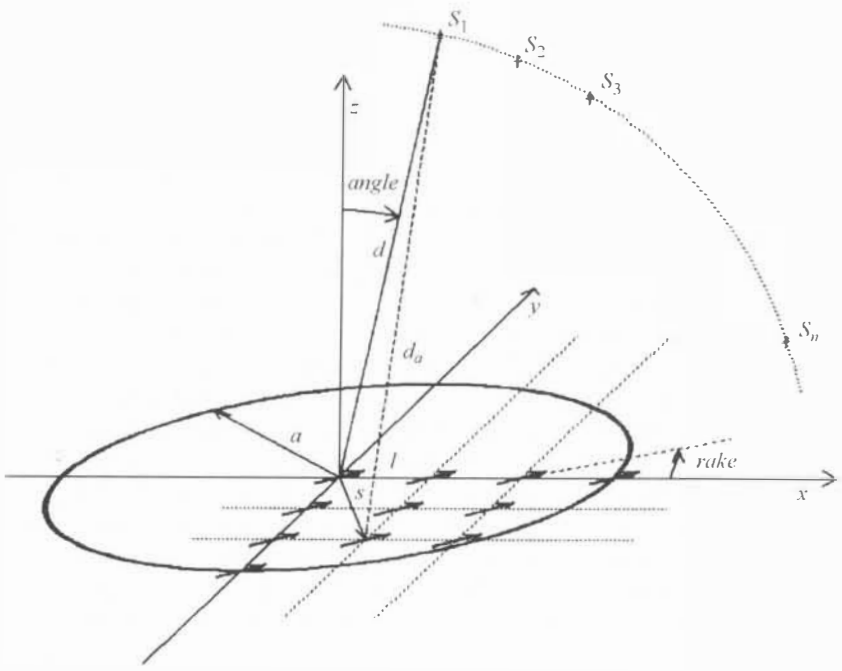

FIGURE 1. The model of the finite circular source. The seismograms are observed at points S_n, which are specified by distance d and take-off angle ν. The sub-sources (marked by arrows) are plotted here only in a part of the fault.
gure: $rake = 45°$; the point
the rectangular grid (dotted lines) with a distance of sub-sources $l = a/3$, where a is the circle radius, s is the distance of a sub-source from the origin, d_{nk} is the distance of a sub-source k from point S_n ($n = 1$).

of seismograms

$$w_n = \sum_k w_{nk} \,. \tag{2c}$$

Formula (2b) is only valid for unbounded homogeneous isotropic media (see below). The seismograms must be integrated before energy evaluat
(1) (to convert displacement into velocity).

Performed tests
tion of sub-STF given as $t_{dur} = t_2 - t_1$ produced a rather symmetric signal of the finite source (the
angles caused by the finite source were rather small and symmetric — see examples in Figs. 4a, b). To emphasise the

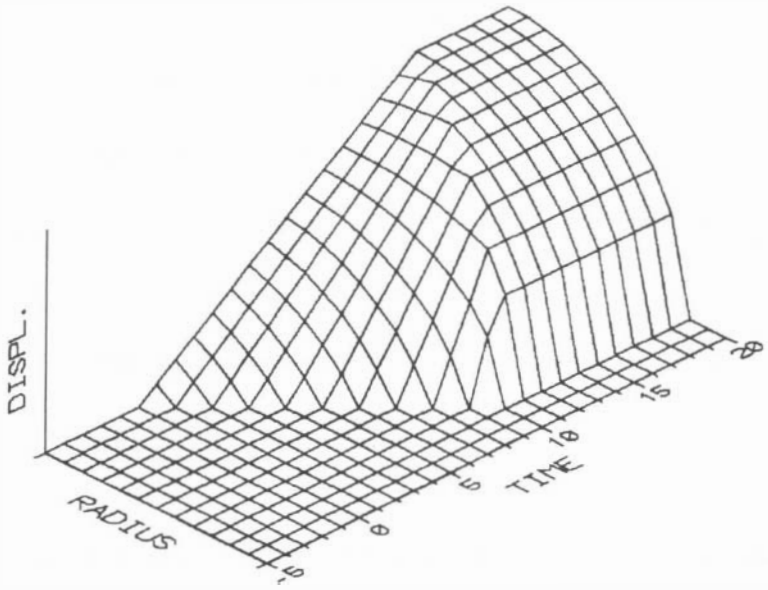

FIGURE 2. A schematic example of the time dependence of displacement on the circular fault. A section along radius a is plotted
$t = 0$ in the centre. The rupture f
fault border at time $t = 10$ and at the same time it turns
centre at time $t = 15$; the figure therefore
the healing process is two times shorter than the rupture process (c.f. formula 3). Amplitudes of the displacement
formula 2a. Notice that for this schematic example simpler slip course given in Fig. 3 curve a was used, instead of a smooth one given by

was arbitrarily shortened according to the formula

$$t_{\mathrm{dur}} = \frac{t_2 - t_1}{1.5} = 2\,\frac{a - s}{v_r}\,\frac{1}{1.5}\,, \tag{3}$$

where $t_1 = s/v_r$. An example of the modification can be seen in Figs. 5a, b.

Notice that the modification of the time duration (formula 3) also roughly corresponds to the formula for the relation between source radius a and corner frequency f_c (or period t_{dur}, respectively) given e.g. by Brune (1970) or Antonini (1987). The formula is

$$a = \frac{2.3 v_S}{2\pi f_c}\,. \tag{4}$$

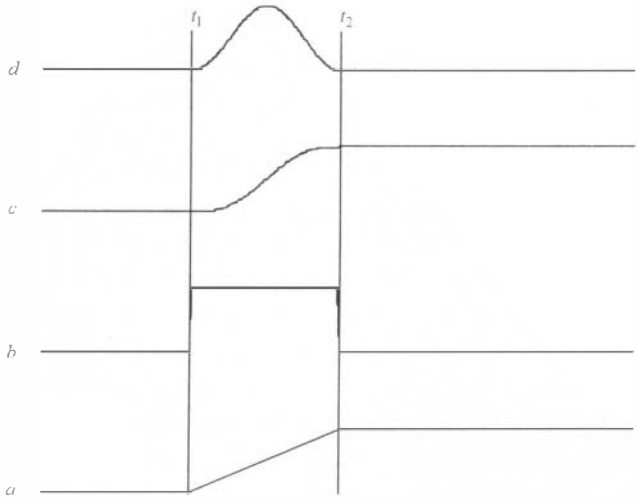

FIGURE 3. Shapes of the displacement
functions;
one an amplitude. The curve a represents a simple
displacement
(t_1) and the
sub-source time f
smoother
sub-source time function
described as one period of

Suppose for a moment, that corner frequency f_c — the highest frequency which is still
decrease by spectrum fall-off) depends on the longest sub-source time function. This sub-STF is radiated by the cent . If
supposed to be inversely proportional to its time duration and $v_S = 3.5\,\mathrm{km/s}$ (see below), then the value of proportionality in for
approximately

The modification of t_{dur} emphasized the
of a synthetic
ν and φ (see the examples in Figs. 4a, b, 5a, b). In this model of the finite source the sub-source situated at the centre radiates the
t_{dur}) with a maximum amplitude ($B = B_0$), the sub-sources at the fault border radiate
Notice, that decay of amplit
steep enough to avoid an infinite increase of radiated energy. It should be stressed, that t
case and there is no need to

For our model of source we used very simple course of slip in the source. However,

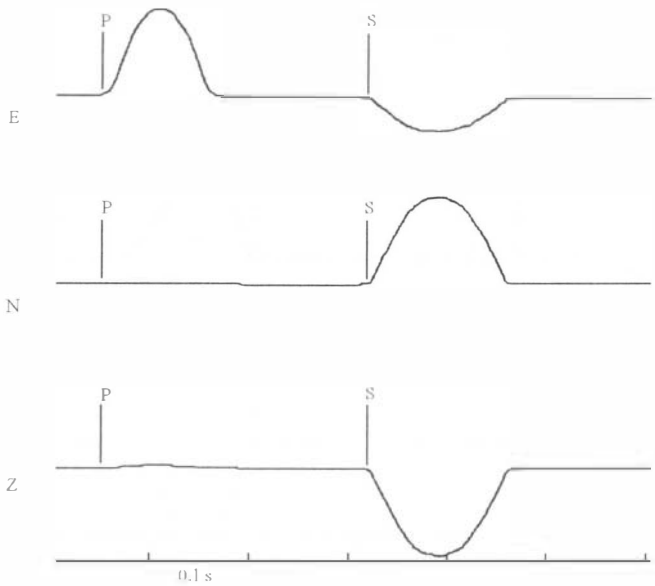

FIGURE 4a. An example of seismogram with non modified time duration t_{dur}. H
45°, distance $d = 10a$, fault radius $a = 0.25$ km, distance of point sources $l = a/10$. In Fig. 4a the take–off angle $\nu = 83.25°$. P and S waves are marked.

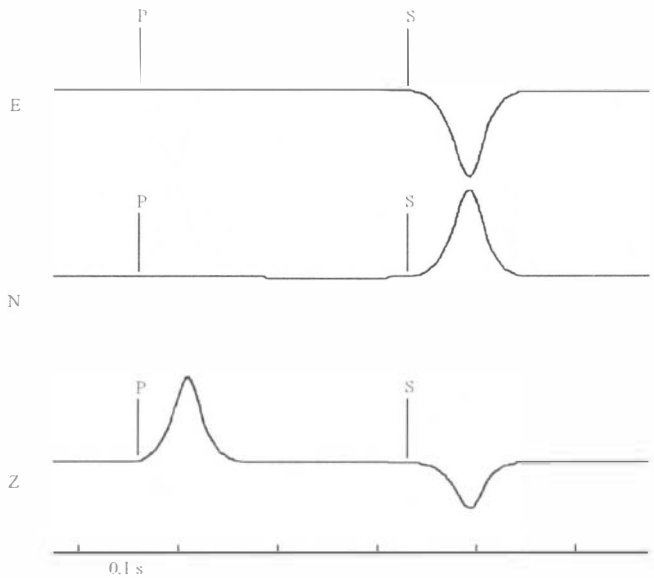

FIGURE 4b. The same as in Fig. 4a, but for the take–off angle $\nu = 6.75°$

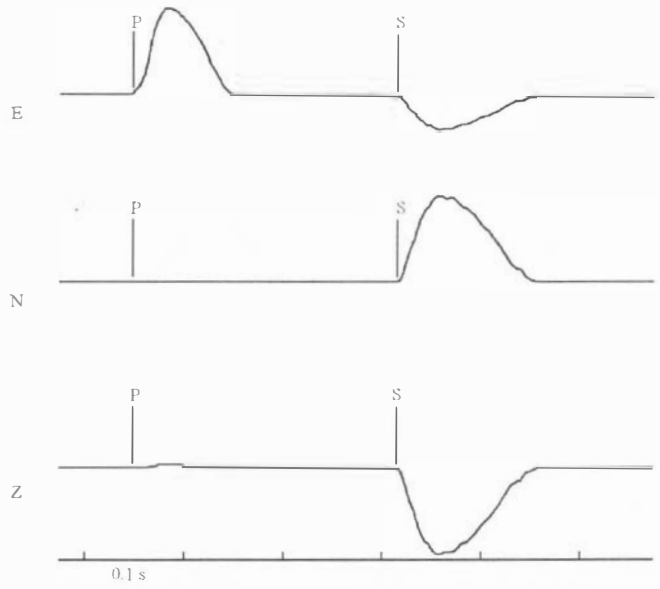

FIGURE 5a. The same as in Fig. 4a, but here the time duration t_{dur} in is modified (shortened) according formula (3). Here, the take–off angle $\nu = 83.25°$. The signal shapes modification as well as time duration changes are evident in comparison with Fig. 4a, b.

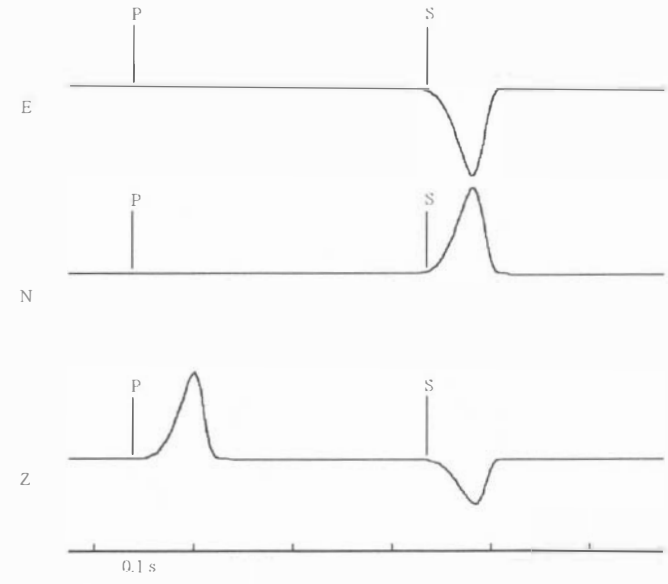

FIGURE 5b. The same as in Fig. 5a, but for the take–off angle $\nu = 6.75°$.

if required, it could be relatively simply replaced in t
courses, which were proposed e.g. by Madariaga (1976) or Boatwright (1980).

Figure 6 shows two examples of the source spectra. From the figure it follows, that corner frequency slightly depends on the take–off–angel and that fall–off of the spectra is about f^{-3} that is more than usual value f^{-2}. Problems with proper spectra fall–off of model of finite sources were discussed e.g. by Fujiwara and Irikura (1991).

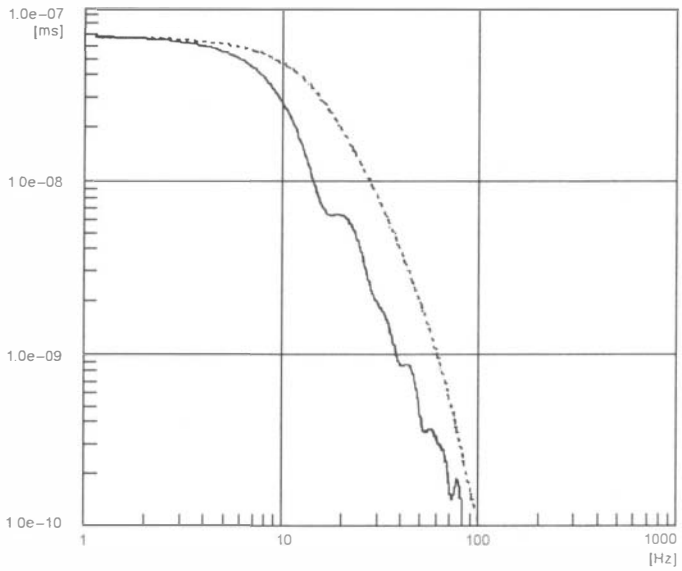

FIGURE 6. Amplitude spectra of P waves of synthetic seismograms in Fig. 5. The spectrum of the E component of the seismogram in Fig. 5a (take–off angle $\nu = 83.25^{\circ}$ — full line) and the spectrum of the Z component of the seismogram in Fig. 5b ($\nu = 6.75^{\circ}$ — dashed line). Notice slight variation of the corner frequency f_r (form about
which is about f^{-3} for both spectra.

3. CALCULATIONS OF SEISMOGRAMS AND SEISMIC ENERGY

In present study I am interested only in particular influence of a finite source and I am not interested in any other effects about which I suppose that they are know and in principle correctable. Therefore I can simplify calculations and consider only an unbounded isotropic homogeneous medium. In such a model the waves from point sources are affected
depends only on the distance between the source and a point of observation (see formula 2b). The values $v_P = 5.76$ km/s, $v_P/v_S = 1.65$, $a = 0.25$ km and $v_r = 0.9 v_S$ were used for calculation. Particular values of v_P, v_P/v_S and a which were used

are taken over from a real situation in which seismic energy was calculated for a set of real events (Kolář, 1994b). However, I would presume that such values could be close or similar to the situation of many places with local events. The given relation for v_r is widely used — see e.g. Madariaga (1976); some other acceptable values of v_r were also tested — see below. The performed numerical tests showed that for distance between points sources of which the final source is composed, it is enough to put $l = 0.1a$ (i.e. $l = 0.025$ km in our case). If the value of l is shorter (i.e. the finite source is represented by larger number of sub–sources), the final seismogram does not change.

The points of observation S_n were situated along the arcs with radius $l = 10a$, $40a$ and $60a$ (i.e. 2.5, 10.0 and 15.0 km in our case). Seismograms were calculated for twenty receivers regularly spread out on the arc in one quadrant (i.e. for take–off angles ν from 2.25° to 87.75° with step 4.5°). The angle ν is measured from the perpendicular line to the plane of the finite source (see Fig. 1). Then energies were calculated from all synthetic seismograms by formula (1) — i.e. a point source is assumed. Since an unbounded isotropic homogeneous medium is supposed, the coefficients A and K are unit and coefficient G is simply inversely proportional to the distance d.

Let me make a few comments on the properties of this source: the final signal, of course, is not monochromatic, however, the distances d given above can be also expressed in wave length λ_0 which corresponds to the length of S wave radiated by the sub–source situated in the centre of the source. The sub–source in the source centre has the longest sub–source time function, i.e. maximal value of t_{4ur}. The distances d are about $6.6\,\lambda_0$, $26.6\,\lambda_0$ and $40.0\,\lambda_0$. Shorter distances d cannot be used as for them the P and S waves are not separated and our method of energy calculation cannot be used then. The change of distance d changes also the ratio of d/a, which can be also understood as a change of radius a for constant distance d: the conclusions about the calculated energy are then similar.

Despite of my attempt, I was not able to determine the radiated energy by an analytical form. Thus, the total radiated energy (which is used for comparison with the energy determined by formula 1) is evaluated by numerical integration over the all sphere. Nevertheless, by numerical experiments it was discovered that the total radiated energy depends on square of maximum central amplitude B_0^2 and on cube of source radius a^3 for our model of the finite circular source. Further I found out that scalar seismic moment M of our source is proportional to square of source radius a^2. As total radiated energy is proportional to a^3, it follows then that the energy is proportional to a M.

4. Results

The influence of several parameters were tested in the course of calculations of seismic energy from seismograms radiated by a finite seismic source; the results are given in this section and plotted in figures 7 – 10. The curves in the figures always show relative changes of seismic energy versus take–off angel ν. The value of total P wave energy really radiated by the finite source was chosen as an unit (remember,

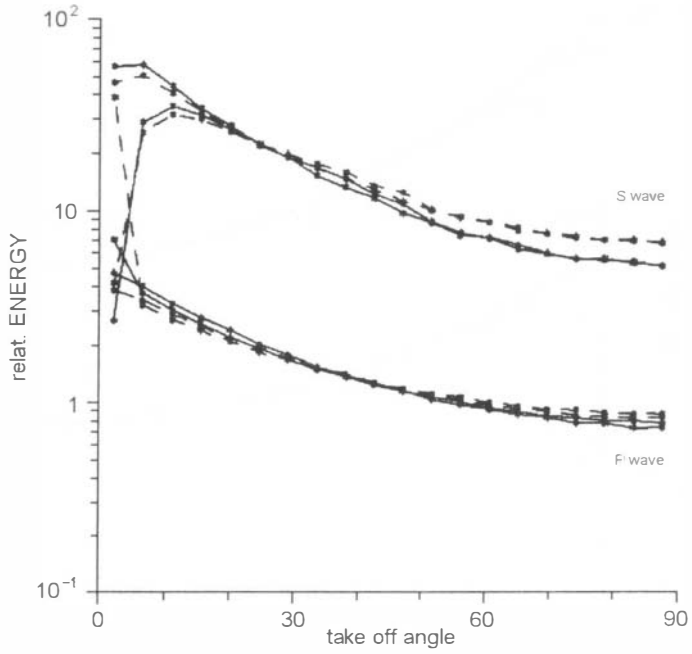

FIGURE 7. Test of the influence of the rupture velocity v_r. In the figure, relative seismic energies of P and S waves (in logarithmic scale) versus take-off angle ν are plotted. Values $v_r = 0.7v_S$ (dashed lines) and $v_r = 0.9v_S$ (full lines) were used: energies were normalized by the value of P waves energy which was determined by numerical integration. For each value of the rupture velocity two lines are plotted for distances $d = 10a$ and $40a$; $rake = 30^o$. The figure shows that results are practically independent on the value of the rupture velocity; the only exception (energy for small take-off angles ν, $v_r = 0.9v_S$ and distance $d = 10a$) quickly vanishes with increasing distance d.

that this value was obtained by numerical integration of energy density of P waves all over the sphere). The curves of P and S energies also show their mutual ratio.

Influence of rupture velocity: for the rupture velocity v_r value $v_r = 0.9v_S$ was accepted (see Sec. 3), however, the acceptable values of v_r can lie in the interval $0.7-0.9v_r$ (Madariaga, 1976). Thus the values $0.7v_r$ and $0.9v_r$ were used for calculations and the results were compared. The result of the test is given in Fig. 7 and shows that the value of the rupture velocity practically does not influence the calculated energy. Therefore, for further calculations only value $v_r = 0.9v_S$ was used. As the test showed that the energy dependence on the v_r is weak, other values from the acceptable interval were not tested.

Influence of distance: the influence of the distance d was tested. As presented

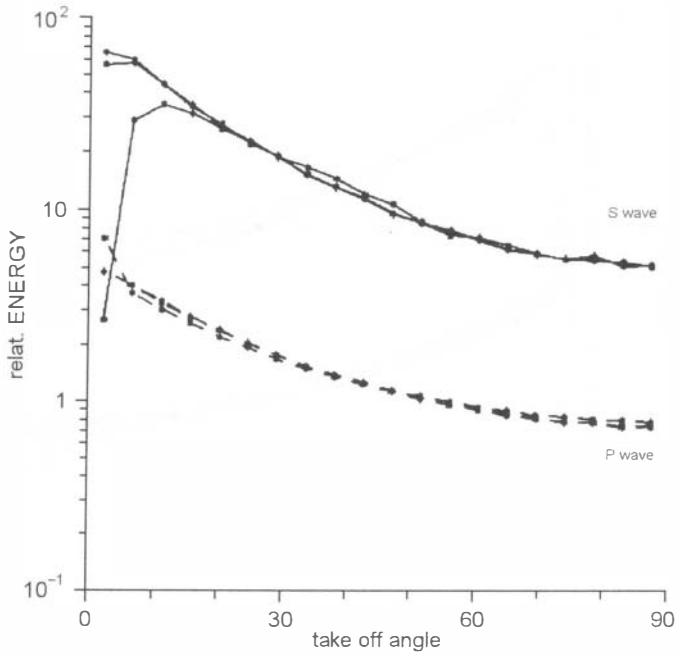

FIGURE 8. Test of the influence of the distance d. In the figure, relative seismic energies (in logarithmic scale) of S waves (full lines) and of P waves (dashed lines) versus take–off angle ν are plotted. Values $v_r = 0.9v_S$ and $rake = 30^o$ were used. The curves correspond to distances $d = 10a$, $40a$ and $60a$. The figure shows that the differences for various values of distance d are none or small. The only exception is the energy of S waves for values of take–off angle ν close to zero. The performed tests showed that this anomalous behaviour vanished if the distance d increased. Values of energies in figure were normalized (as in Fig. 7) by the value of P waves energy.

above, the values $d = 10a$, $40a$ and $60a$ were used. The performed tests showed that in general the distance changes did not have an important influence on seismic energy (see Fig. 8). The anomaly of energy for the take–off angle close to 0^o is not very important; it occurs only for small distance d, and quickly vanishes with its increase.

Influence of rake: the last parameter under the test was rake. It was considered from the interval of $0^o - 90^o$ (other values are complementary to this interval). The step was maximum 5^o and at places with anomalous behaviour even shorter (e.g. 2^o). There are no changes in the (relative) seismic energy for most values of the interval, however, there is again an exception. For values of rake close to zero (i.e. double–couple oriented approximately in the direction of the plane in which points

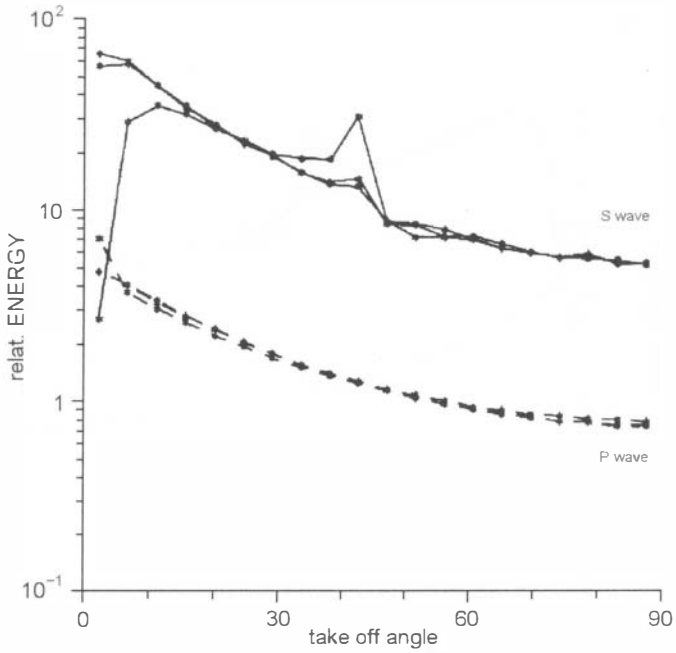

FIGURE 9. An example of anomalous behaviour of the (relative) seismic energy of S waves (full lines). In the figure, relative seismic energies for distances $d = 10a$, $40a$ and $60a$ for $rake = 0°$ are plotted. The figure shows that there is an anomalous behaviour of S waves energies in the interval of the *take–off angle* of $40° - 50°$. The greatest values of the anomaly corresponds to smaller distances d; the value of the anomaly never exceed a range in which other values of the relative energy lie. For the energy of P waves (dashed lines) no anomalies are observed. Values of energies in figure were normalized (as in Fig. 7) by the value of P waves energy.

of observation
waves for some take–off
example for different d is given in Fig. 9. Tests showed that amplitudes of the anomaly increased if the distance d was small and decreased with increasing rake. The dependence of the anomaly on the parameter rake is shown in Fig. 10.

The method of determinatio
required knowledge of plenty of information and of course the result precision depends on the reliability of these knowledge. Judging according to our experience with real earthquake processing (Kolář, 1992; 1994a; b), we suppose that
t
termination of radiated energy is performed. In other
corrected all other influences (included in formula 1), i.e. if we know all the nec-

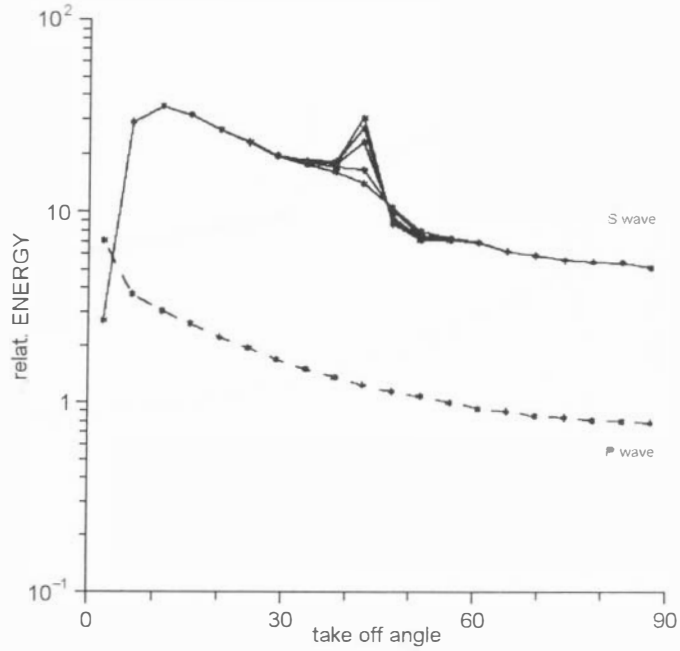

FIGURE 10. Comparison of the influence of the parameter *rake* on the anomalous behaviour of the energy. The curves are plotted for distance $d = 10a$ and for *rake* $= 0^\circ, 2^\circ, 5^\circ, 10^\circ, 15^\circ$. There is no anomaly for P waves energy (dashed line). For S wave energy (full lines) there is an anomaly for *take–off angles* ν from interval $40^\circ - 60^\circ$. The anomalies do not exceed an order of magnitude and their amplitudes decrease with increasing *rake*. For *rake* $= 15^\circ$ the curve is already practically monotonous. Values of energies in figure were normalized (as in Fig. 7) by the value of P waves energy.

essary information. Unfortunately, it is probably not a very common case for real data. Moreover, to perform such a correction we must know or suppose the diameter of finite source in addition to all others required information.

5. CONCLUSION

From the performed numerical tests it follows, that the neglecting of influence of finite seismic source can affected the determined seismic energy. However, the differences are within an order of magnitude. The influence of *take–off angle* was found as the most affective among tested parameters. Other investigated parameters (*distance* and *rake*) have less importance: there is almost no influence of *rupture velocity*. The dependency of determined energy on *take–off angle* is monotonous in general, however some irregularities for S waves energy were discovered.

The by-product of the work is a simple kinematics model of a finite circular (double-couple) seismic source, which could be also suitable for some other future calculations. It has been found out that some properties of our source model (namely spectrum fall-off) do not meet fully the general demands on a final source model. This effect is consequence of our extremely simple course of slip on the fault area. If necessary, model can be completed by more sophisticated displacement courses designed by others authors (see above).

References

Aki K. and Richards P.G.: 1980. *Quantitative Seismology Theory and Methods.* (W. H. Freeman and Company, San Francisco).

Antonini M.: 1987. Statistic and Source Parameter of the Swarm from Digital Recordings. In: *Earthquake Swarm 1985/86 in Western Bohemia* (D. Procházková, ed.) Geophys. Inst. of Czechosl. Acad. Sci., Prague, pp. 205–217.

Boore D.M. and Boatwright J.: 1984. Average Body-wave Radiation Coefficients. *Bull. seism. Soc. Am.* **74**, pp. 1615–1621.

Brune J.N.: 1970. Tectonic Stress and the Spectra of Seismic Shear Waves from Earthquakes. *J. Geoph. Res.* **75**, 4997–5009.

Boatwright J.: 1980. A Spectral Theory for Circular Seismic Sources; Simple Estimation of Source Dimension, Dynamic Stress Drop and Radiated Seismic Energy. *Bull. seism. Soc. Am.* **70**, 1–27.

Fujiwara H. and Irikura K.: 1991. High-frequency Seismic Wave Radiation from Antiplane Cohesive Zone Model and f_{max} as Source Effect. *BSSA* **81**, No.4, pp.1115–1128.

Golicyn B.B.: 1915. *O zemletrasenii 18 fevralja 1911g.* In: Izd. Ross. Akad. Nauk. 1915, 9, No.10, or also: Izbranie trudy, Izdatelstvo AN CCCP, 1960, tom II., Moscow, 365–370. (in Russian)

Kolář P.: 1992. *Energy of Seismic Waves.* Ph.D. thesis, Geophys. Inst. of Czechosl. Acad. Sci., Prague. (in Czech)

Kolář P.: 1994a. Energy of Selected Events of 1985/86 West-Bohemian Earthquake Swarm. *Studia Geophys. et Geod.* **38**, 23–36.

Kolář P.: 1994b. Simultaneous Determination of the Source Mechanism and the Seismic Wave Energy. *Pageoph* **143**, 655–671.

Madariaga R.: 1976. Dynamics of an Expanding Circular Fault. *Bull. seism. Soc. Am.* **66**, 639–666.

Energie seismických vln vyzářených konečným zdrojem — numerický přístup

Petr KOLÁŘ

Používáme metodu, která umožňuje určení energie vyzářené v seismických vlnách ze seismogramu zaznamenaného pouze na jedné stanici. Tato metodika byla navržena Golicynem (1915) a modifikována Boatwrightem (1980). Výpočet je založen na integraci (kvadrátu) záznamu rychlosti, který je následně opraven o vliv prostředí, vyzařovací charakteristiku zdroje, atd. Integrací takto určené hustoty toku energie přes fokální sféru pak získáváme celkovou vyzářenou energii.

Již dříve jsme prováděli výpočty energie pomocí této metody pro vybrané jevy ze západočeské zemětřesné oblasti (Kolář, 1992; 1994a; b). V předkládané práci se zaměřujeme pouze na jeden aspekt metody a porovnáváme, jak se určená energie

může lišit, jestliže při výpočtu zanedbáme konečnost zdroje a nahradíme jej zdrojem bodovým. Problém byl zkoumán pomocí numerických experimentů. Abychom byli schopni konstruovat příslušné syntetické seismogramy, navrhli jsme jednoduchý kinematický model konečného seismického zdroje. Náš zdroje je rovinný kruhový a je tvořen superpozicí pravidelně rozmístěných bodových sub–zdrojů typu dvojitého dipólu. Navrhli jsme rovněž časovou funkci zdroje a průběh procesu trhání na zlomu.

Při výpočtech jsme postupovali následovně: spočetli jsme syntetické seismogramy generované námi navrženým konečným zdrojem. Z těchto seismogramů jsme pak (za předpokladu bodového zdroje) určovali seismickou energii výše zmíněnou metodou. Takto získanou hodnotu energie jsme porovnávali se správnou hodnotou energie, která byla určena přímou integrací všech seismogramů vyzářených konečným zdrojem. V průběhu práce jsme sledovali vliv *úhlu východu* paprsku ze zdroje, *vzdálenosti*, *rake–u* a *rychlosti trhání* na celkovou hodnotu určené energie. Zjistili jsme, že zanedbání konečného zdroje může ovlivnit hodnotu určené energie, rozdíly jsou však menší než jeden řád. Vliv hodnoty *úhlu východu* se ukázal jako nejvýznamnější, vliv hodnot ostatních zkoumaných parametrů (tj. *vzdálenosti*, *rake–u*, *rychlosti trhání*) je menší. Závislost určené energie na *úhlu východu* je všeobecně monotonní, avšak objevili jsme několik neregulárností pro *S* vlny.

Ke stanovení energie seismických vln pomocí použité metody stačí pouze jeden seismogram, je však nutno mít k dispozici mnoho dalších údajů (o prostředí, mechanismu zdroje, atd.). Při praktickém použití metody jsou často tyto nezbytné údaje známy pouze přibližně. Soudíme, a to i na základě naší dřívější zkušenosti se zpracováním reálných dat, že vzhledem k těmto nepřesnostem a chybám může mít korekce vlivu konečného zdroje význam pouze při velmi detailním určování seismické energie, které ale nebude pro reálná data pravděpodobně příliš často prakticky realizovatelné.